PROCEEDINGS, Thirty-Eighth Workshop on Geothermal Reservoir Engineering
Stanford University, Stanford, California, February 11-13, 2013
SGP-TR-198

A STUDY ON PRESSURE AND TEMPERATURE BEHAVIORS OF GEOTHERMAL WELLS IN SINGLE-PHASE LIQUID RESERVOIRS

Yildiray Palabiyik, O. Inanc Tureyen, Mustafa Onur and Melek Deniz

Istanbul Technical University
ITU Petroleum and Natural Gas Eng. Dept.
Maslak, Istanbul, 34469 TURKEY
e-mail: palabiyiky@itu.edu.tr, inanct@itu.edu.tr, onur@itu.edu.tr and denizmel@itu.edu.tr

ABSTRACT

In this study, a non-isothermal reservoir simulator that is capable of rigorously simulating (or forwarding) both pressure and temperature behaviors of single-phase liquid-dominated geothermal systems is presented. The model is based on solving the mass and energy balance equations for the reservoir simultaneously. The model is also capable of simulating heat losses from the reservoir to the strata enabling realistic simulations of temperature to be made in the well. All equations are solved in a fully implicit manner using the well-known Newton's method for handling the non-linearity. The model is 2D (*r*-*z*) cylindrical and hence provides realistic descriptions of wellbore pressure and temperature behaviors. The transient behaviors of especially temperature, which is the main focus of the study, and various sensitivities of formation and well properties on the pressure and temperature responses have been studied by using the model developed. The synthetic examples considered in this study have shown that the wellbore temperature shows the most significant sensitivity to rock thermal conductivity among the other parameters, such as porosity, skin and permeability, considered for this investigation.

INTRODUCTION

Temperature measurements, though routinely recorded in well test applications, are usually ignored in reservoir characterization. However, the investigation of temperature data for the purpose of reservoir characterization has recently attracted the attention of various researchers. Temperature measurements in addition to pressure data have been shown to aid in reservoir characterization. The main objective of this study is to further investigate the temperature behavior (at a well and observation points) of single-phase liquid-dominated geothermal systems for the reservoir characterization, especially under constant and variable rate production and injection scenarios by a non-isothermal single-phase simulator developed during the course of this study.

The use of temperature measurements for geothermal reservoir characterization requires a forward model which is capable of simulating the temperature behavior of a geothermal system. Geothermal reservoirs are usually modeled by using two approaches. These are distributed models and lumped parameter models. Various versions of the lumped parameter models, assuming isothermal flow behavior, have been proposed by Grant et al., (1982), Axelsson, (1989), Alkan and Satman, (1990), Sarak et al., (2005) and Tureyen et al., (2007). Onur et al. (2008) have proposed a non-isothermal lumped-parameter model which enables one to predict both pressure and temperature behaviors of a single-phase liquid-dominated geothermal reservoir which is idealized as a single-closed or recharged tank. Onur et al. (2008) show that one could determine reservoir parameters such as reservoir bulk volume and porosity if the information content of average reservoir temperature data is combined with average pressure data in history-matching. Then, Tureyen et al. (2009) extended the lumped model proposed by Onur et al. (2008) to study for multiple tanks. However, since the lumped parameter modeling was used in these studies, spatial changes in pressure and temperature along with their sensitivities to various formation and well properties (e.g., permeability, porosity, skin, etc.) cannot be modeled and investigated by such models. In this study, such transient behaviors and sensitivities of the pressure and temperature at the production/injection locations at the wellbore and observation points along the wellbore and inside the reservoir are investigated by developing a more realistic simulator.

The most of the models based on the analytical and semi-analytical solutions assume that the rock and fluid properties appearing in the mass and heat balance equations are independent of pressure and

temperature. Under these assumptions, it becomes possible to solve the mass balance equation independent of the heat flow equation analytically or semi-analytically. The earlier analytical solutions are given by Atkinson and Ramey (1972) who presented the analytical solutions for several problems to predict temperature behavior in the reservoir under various simplifying assumptions (e.g. rock/fluid properties independent of pressure and temperature, uniform fluid velocity inside the reservoir, etc.).

The latest studies focusing on the analytical and semi-analytical solutions on this topic have been presented by Ramazanov et al. (2010), Duru and Horne (2010a), and Duru and Horne (2011). Ramazanov et al. (2010) have used the method of characteristics to calculate temperature behavior, whereas Duru and Horne (2010a, 2011) have modeled pressure and temperature behaviors by using the method of operator-splitting and time stepping. Both solutions are semi-analytical as they require time stepping to evaluate the solutions. The important advantage of the method presented by Duru and Horne (2010a, 2011) in comparison with the model of Ramazanov et al. is that Duru and Horne (2010a, 2011) consider both effects of the conductive and convective heat transfers in reservoir, whereas Ramazanov et al. considered only the convective heat transfer in the reservoir. In these studies, it has been shown that important information about reservoir permeability and porosity along with skin zone can be obtained from temperature measurements. Furthermore, Duru and Horne (2010a) have also shown that production rate data from temperature data could be predictable. However, as Ramazanov et al. have also mentioned, the conclusions above is for the cases where the wellbore storage effects could be negligible and flow rates are very high. Therefore, they have recommended that the more general numerical solutions be used to obtain the more accurate temperature solutions.

Studies of App (2008) and Sui et al. (2008a, b) can be given as the examples of numerical models considered important in the literature regarding the topic of this study. App (2008) have developed a transient, 1D radial model coupling the conservation of mass and energy equations for predicting the pressure and temperature behaviors of a system that has the components oil, connate water and rock. In that study, the pressure and temperature behavior under non-isothermal conditions in the reservoir due to Joule-Thomson expansion of reservoir fluids has been presented. Sui et al. (2008a) developed a 2D (*r*-*z*) radial simulator to study temperature behavior for the case of single-phase liquid flow in 2D stratified systems. In the study, the improved energy balance equation has been formulated in a general way to contain the effects like Joule-Thomson and thermal expansion, while the temporal and spatial variations of pressure required in energy balance equation have been calculated from the mass (pressure) balance equation developed under the assumptions of isothermal flow and slightly compressible fluid. This assumption is essentially the one used in the semi-analytical solutions of Ramazanov et al. (2010) and Duru and Horne (2010a). Hence, these solutions cannot rigorously model the pressure and temperature behavior under non-isothermal conditions. The most important finding of Sui et al. (2008a) is that in stratified systems, the wellbore temperature is sensitive to the radius and permeability of damage zone near the wellbore. In their second study, Sui et al. (2008b) presented an algorithm for an inverse solution formulated as a non-linear least-squares regression problem to estimate permeability (region outside damage zone), porosity, radius and permeability of damage zone by history matching observed temperature and pressure data. Sui et al. (2008b) reported that the related parameters could reliably be estimated by history matching temperature data if noise in temperature measurements is not very high.

Another study regarding the information content of transient temperature data has been conducted by Duru and Horne (2010b). In this study, inverse solution of permeability and porosity distributions in reservoir were investigated by history matching to temperature data with the method of Ensemble Kalman Filter (EnKF) by using a forward model based on coupled numerical solution of mass and energy balance equations for a 3D (*x*-*y*-*z*) system. The main conclusion of the study was that temperature data contain more information about porosity distribution than that of permeability distribution.

As mentioned, the objective of this study is to investigate the behaviors and sensitivities of the pressure and temperature at the production/injection locations at the wellbore and observation points along the wellbore for a single-phase liquid geothermal reservoir. For this purpose, a 2D (*r*-*z*) fully implicit numerical model avoiding the limitations of the analytical, semi-analytical models and some of the numerical solutions (e.g., those of Sui et al.) mentioned above.

The paper is organized as follows: First the development of the model will be provided. This will be followed by the verification of the model through comparison with a well-known commercial simulator. Then, we provide cases where the effects

of various reservoir and well properties on the pressure and temperature are illustrated.

DEVELOPMENT OF THE MODEL

The numerical simulator developed during the course of this study rigorously accounts for mass, Darcy's equation and energy balances to include convection and conduction heat transfers to adjacent strata. Heat transfer to adjacent strata is modeled by assigning temperature gradients to overburden and underburden strata in *z*-direction. The model simulates pressure and temperature behaviors resulting from production of hot water and/or injection of low temperature water into reservoir and enables handling variable production and injection rate histories.

The non-linear mass and energy balance equations are solved by using the well-known Newton's method in a fully implicit manner. The model simulates the behavior of pressure and temperature and investigates sensitivities of formation and well properties on the pressure and temperature responses. In the following subsections, we will briefly describe the main equations used in developing the 2D (*r*-*z*) simulator, and the detailed derivation of finite difference equations will not be presented here and can be found in Palabiyik (2013).

Reservoir Equations for the Model

Mass and energy balance are solved for the rock and for the liquid phase. The partial differential equation that describes mass conservation in *r*-*z* coordinates is given by

$$\frac{\partial(\rho_w\phi)}{\partial t}+\frac{1}{r}\frac{\partial}{\partial r}(\rho_w r v_r)+\frac{\partial}{\partial z}(\rho_w v_z)=0 \qquad (1)$$

Following Bird et al. (1960) the partial differential equation describing energy conservation is given by

$$\frac{\partial}{\partial t}\left[\phi\rho_w U_w+(1-\phi)\rho_s C_{p,s}T\right] = -(\nabla\bullet\rho_w H_w\vec{v}_w)-(\nabla\bullet\tilde{q}) \qquad (2)$$

The term on left hand side of Equation 2 defines temporal accumulation of internal energy per unit reservoir volume. The first term on right hand side of Equation 2 represents heat transfer transported with fluid flow due to convection. The second term represents heat transfer into the cell via conduction. All symbols and their units used in Equations 1 and 2 are given in the Nomenclature section.

In this modeling study, gravity effect in *z*-direction is ignored and local thermal equilibrium between solid rock and fluid phases is assumed because heat is stored in both solid rock and fluid.

Equations 1 and 2 are discretized by considering gridblock representation shown in Figure 1 where r_i, θ_j, z_k is the geometric center of the *i*, *j*, *k* gridblock. Although the representation shown in Figure 1 consider a three-dimensional flow, we will consider flow only in the *r* and *z* directions.

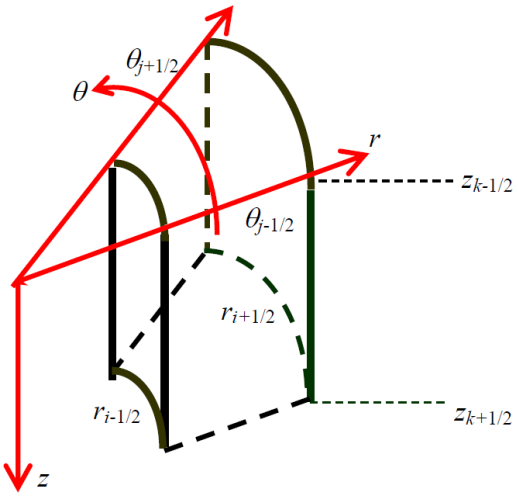

Figure 1: 3D (r-θ-z) gridblock illustration.

Well Equations for the Model

Mass and thermal conservation equations should be used for inner boundary (wellbore) conditions for pressure and temperature. For example, the equation of inner boundary condition for wellbore production/injection rate can be written for the system shown in Figure 2 as follows:

$$V^w\frac{\partial(\rho_w^w)}{\partial t}=(\rho_w^w q_z^w)_{z=0}+q_m^R \qquad (3)$$

Here, subscript "*w*" and superscript "*w*" are used to represent water and well, respectively. In Equation 3, V^w and q_z^w represent wellbore volume of well (from *z* = 0 to bottom hole) and volumetric water flow rate in the wellbore at the level of *z* = 0, respectively. While q_z^w is taken as $q_z^w < 0$ for production case from the wellbore, q_z^w is taken as $q_z^w > 0$ for injection case from the wellbore and $q_z^w = 0$ for shut-in case. In Equation 3, q_m^R is source term and represents mass rate in from reservoir into wellbore:

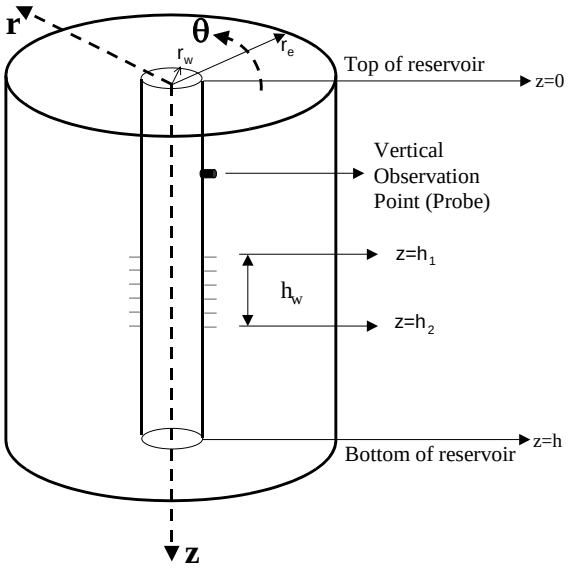

Figure 2: 3D (r-θ-z) view of wellbore/reservoir model with single cell.

$$q_m^R = \left(\rho_w q_{sf}\right)_{r=r_w, h_1 \le z \le h_2} = 2\pi \int_{h_1}^{h_2} \left[\rho_w(z,r) \frac{k_r(r,z)}{\mu_w(r,z)} r \frac{\partial p}{\partial r} \right]_{r=r_w,z} dz \quad (4)$$

If heat losses with convection and conduction and energy loss term due to viscous dissipation in z-direction are ignored in wellbore model given in Figure 2, the thermal conservation equation in the wellbore can be written as follows:

$$V_w^w \frac{d}{dt}\left(\rho_w^w U_w^w\right) = \left(\rho_w H_w q_{sf}\right)_{r=r_w, h_1 \le z \le h_2} + \left(\rho_w^w H_w^w q_z^w\right)_{0 \le r \le r_w, z=0} - 2\pi r_w \hat{U}\left(T^w - T\left(r_w^+, z\right)\right) \quad (5)$$

In this study, the accumulation term on the left hand side of Equation 5 approximates to zero because the well is treated as source or sink. The last term on right hand side of Equation 5 considers heat losses along with convection and conduction between wellbore and reservoir and $\hat{U}$ is overall heat transfer coefficient for the system (Ramey, 1962). In this study, heat transfer along with convection and conduction between wellbore and reservoir is ignored. This means that overall heat transfer coefficient is assumed to be zero.

Outer Boundary and Initial Conditions

To complete the system of equation, we need to impose outer boundary conditions. Our formulation is general in that we can consider both no-flow and constant pressure outer boundaries as well as no-heat flux or constant temperature conditions at the reservoir boundaries.

Regarding initial conditions, we can consider uniform or non-uniform initial pressure (p^0) and temperature (T^0) distributions.

VERIFICATION OF THE MODEL

In this section, the verification of the model developed is conducted through comparison with the commercial thermal software PetraSim which is based on the well-known reservoir simulator Tough2 (Pruess et al., 1999) using different scenarios of production and injection. Here, the developed model has been verified in a 2D (*r-z*) closed (no-flow and no-heat flux) reservoir system in respect of pressure and temperature at the outer boundary (at $r = r_e$) of the reservoir. Heat transfer from reservoir to adjacent strata (at $z = 0$ and $z = h$) has also been included into the systems for both verification and application (to be discussed in the next section) cases. However, at least for the cases considered here, it has been observed that heat transfer to adjacent strata does not have any significant effect on pressure and temperature behaviors. In the verification and application cases, well is treated as a source or sink where its volume is assumed so small for the two simulators (the model developed and PetraSim).

Constant-Rate Injection Case

This scenario contains a constant mass rate of 1 kg/s injection with an injection temperature of 333.15K for a fully penetrating vertical well. The other pertinent reservoir parameters used in this case are given in Table 1.

Table 1: Reservoir data for 2D (r-z) system.

Parameter	Value
N_r	20
N_z	9
P^0, kPa	10000
T^0, K	413.15
r_w, m	0.1
r_e, m	1000
h, m	100
ϕ	0.2
k, m^2	1×10^{-13}
c_s, 1/kPa	2.9×10^{-7}
β_s, 1/K	0
$C_{p,s}$, J/m^{3}K	2.65×10^6
λ_t, J/msK	2.92
q_m, kg/s	1

Figures 3 and 4 show pressure and temperature behaviors along radial distance in reservoir for model and PetraSim, respectively. As can be seen from the figures, both pressure and temperature behaviors from the two different simulators exhibit an excellent agreement for all time periods (from 2×10^{-5} day to 1000 days).

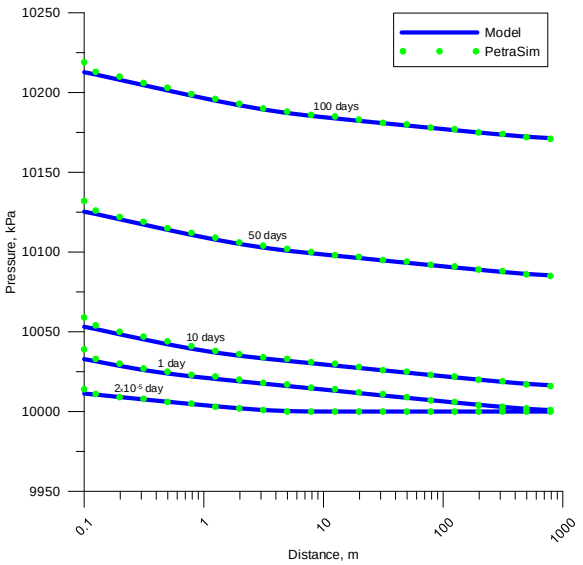

Figure 3: Comparison of pressure behaviors along radial distance in reservoir for the model and PetraSim during constant rate injection period.

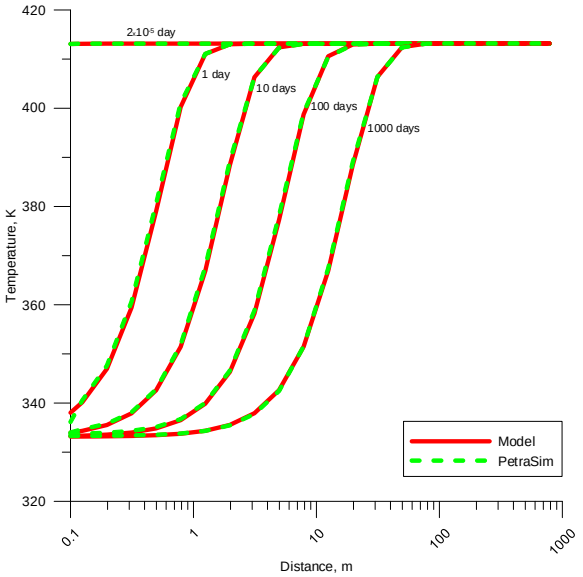

Figure 4: Comparison of temperature behaviors along radial distance in reservoir for the model and PetraSim during constant-rate injection period.

Figures 5 and 6 show wellbore pressure and temperature behaviors with respect to time for model and PetraSim, respectively. As can be seen from the figures, both pressure and temperature behaviors from the two different simulators exhibit a very good agreement.

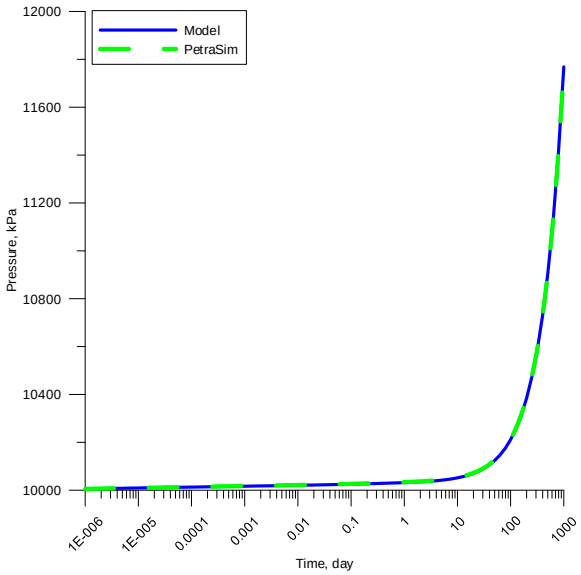

Figure 5: Comparison of wellbore pressure behaviors for the model and PetraSim as a function of time during constant-rate injection period.

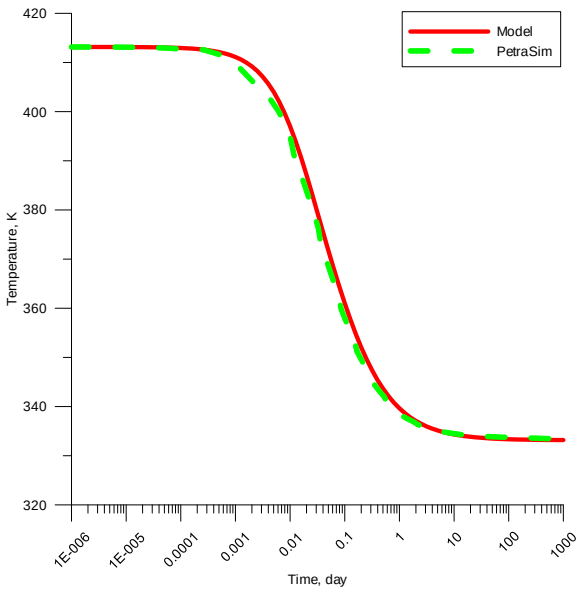

Figure 6: Comparison of wellbore temperature behaviors for the model and PetraSim as a function of time during constant-rate injection period.

Constant-Rate Production Case

Here, a production scenario with a constant mass rate of 1 kg/s has been performed for a fully penetrating vertical well during a time period of 1000 days. The pertinent reservoir parameters used in this case are the same as Table 1.

Figures 7 and 8 show wellbore pressure and temperature behaviors with respect to time for model and PetraSim, respectively. As can be seen from the figures, both pressure and temperature behaviors from the two different simulators exhibit an excellent agreement.

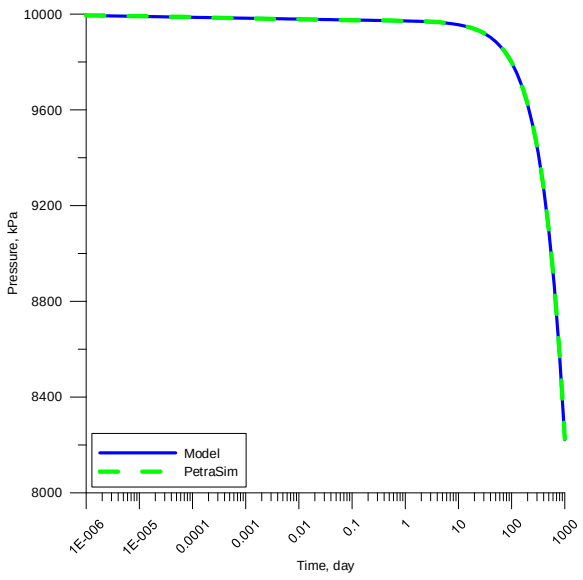

Figure 7: Comparison of wellbore pressure behaviors for the model and PetraSim as a function of time during constant-rate production period.

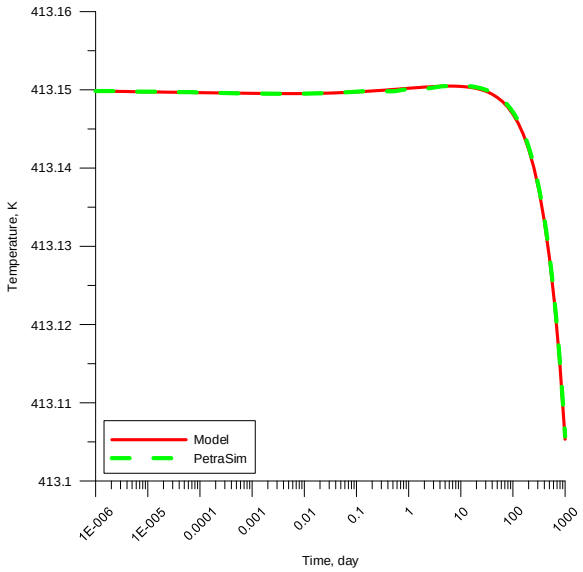

Figure 8: Comparison of wellbore temperature behaviors for the model and PetraSim as a function of time during constant-rate production period.

APPLICATIONS WITH THE MODEL

In this section, various synthetic case studies simulated with the developed model in the 2D (*r*-*z*) reservoir system for predicting both pressure and temperature behaviors of geothermal reservoirs containing single-phase liquid water are presented. Production and injection cases have been modeled for a system with a closed outer boundary. Closed outer boundary condition in the *r*-direction indicates no-flow and no-heat flux (insulated) system in respect of pressure and temperature at the outer boundary (at $r = r_e$) of the reservoir. Heat transfer from reservoir to adjacent strata (at $z = 0$ and $z = h$) has also been included into the system. In none of the cases, anisotropy is not taken into consideration (horizontal and vertical permeabilities are the same). Sensitivities of rock parameters like porosity, permeability, skin factor to pressure and temperature responses have been investigated. The effects of well completion (fully penetrating or limited entry) are also considered. Effects of different intervals for a well having limited entry and effects of different injection temperatures on pressure and temperature behaviors for a limited entry well are also discussed. Parameters given in Table 1 are also used in the application cases unless otherwise stated.

Sensitivity of Pressure and Temperature Behaviors to Rock Thermal Conductivity

In this subsection, sensitivity of pressure and temperature to rock thermal conductivity is investigated for an injection-falloff case. Figure 9 shows pressure behaviors of a fully penetrating well in the reservoir that has different values of rock thermal conductivity during an injection-falloff case. In this case, an injection is performed at constant mass rate of 1 kg/s during 1 day and then, the well is shut in for another 1 day period. According to Figure 9, the effect of rock thermal conductivity on pressure behavior is negligible.

Figure 10 shows temperature behaviors for the same case. In contrast to pressure behavior, temperature behavior is significantly affected by change of values of rock thermal conductivity during both injection and fall-off periods. It can be seen from Figure 10 that temperature drop decreases as rock thermal conductivity increases during injection period. On the other hand, temperature values for all cases increase during fall-off period because fall-off is a conduction dominated process.

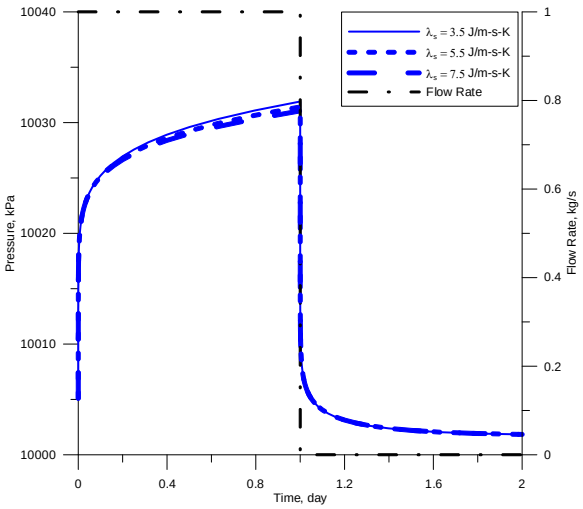

Figure 9: Effect of rock thermal conductivity on wellbore pressure behavior as a function of time during injection and fall-off periods.

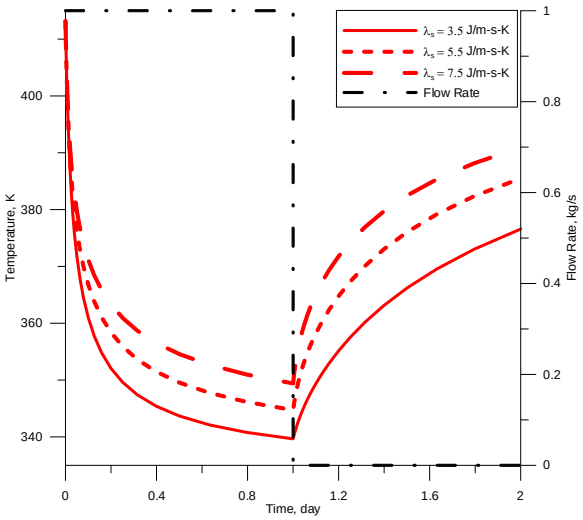

Figure 10: Effect of rock thermal conductivity on wellbore temperature behavior as a function of time during injection and fall-off periods.

Sensitivity of Pressure and Temperature to Porosity

In this subsection, sensitivity of pressure and temperature to porosity is investigated for constant-rate production, injection-falloff and packer-probe cases.

Constant-rate production case

Shown in Figure 11 are the pressure drawdown behaviors of a fully penetrating well in the reservoir that have different porosity values during constant rate production of 1000 days. According to Figure 11, pressure drop increases as porosity decreases. This is an expected result because a reservoir having higher porosity value has more fluid to store and support the pressure drop caused by withdrawal of a certain amount of fluid from the reservoir. Hence, as seen from Figure 11, pressure drop in reservoir having lower porosity (0.04) is much higher than that of higher one (0.2) especially at late time.

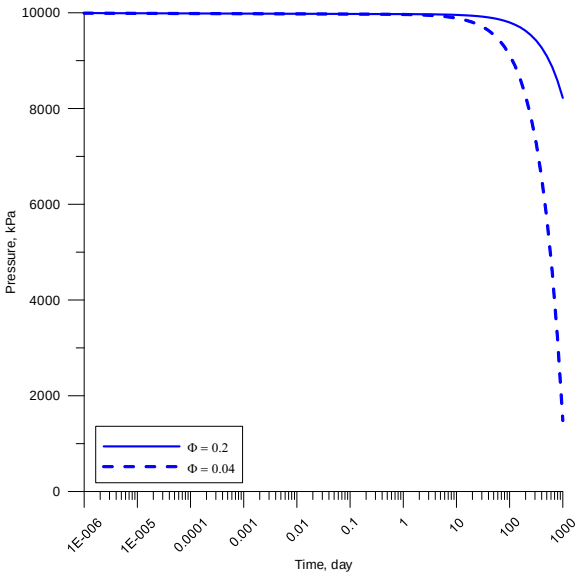

Figure 11: Effect of porosity on wellbore pressure behavior as a function of time for a constant-rate production case.

Figure 12 shows temperature behaviors for the same case. According to Figure 12, temperature has higher values as porosity decreases in contrast to pressure behavior. This is caused by the fact that reservoir having lower porosity has higher heat content than that of reservoir having higher porosity. As is known, most of the heat content in a reservoir (approximately 90% of heat content) is stored in rock while much less amount of heat content is stored in water. However, porosity does not have much effect on temperature in comparison with pressure for the constant-rate production case when the magnitudes of the values are evaluated.

Injection-falloff case

Figure 13 presents pressure behaviors of a fully penetrating well in the reservoir that have different porosity values during an injection-falloff case. In this case, an injection is performed at constant mass rate of 1 kg/s during 1 day and then, the well is shut in for another 1 day period. As expected, pressure has higher values during injection and fall-off periods for lower porosity.

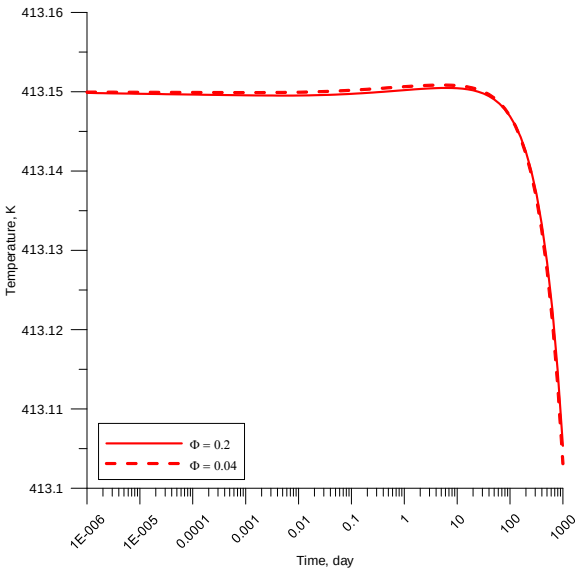

Figure 12: Effect of porosity on wellbore temperature behavior as a function of time for a constant-rate production case.

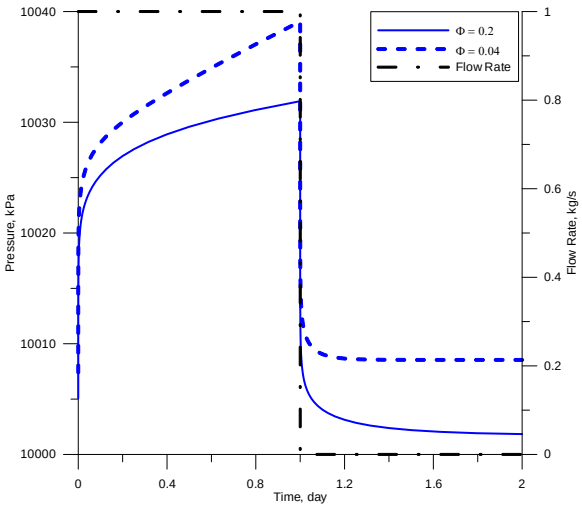

Figure 13: Effect of porosity on wellbore pressure behaviors as a function of time during injection and fall-off periods.

Figure 14 shows temperature behaviors for the same case. Temperature is higher during injection and fall-off periods for a low porosity than that for a large porosity. The sensitivity of temperature to porosity exists for the fall-off period because conduction process dominates over the convection process during fall-off period. Furthermore, the total thermal conductivity $[\lambda_t = \phi\lambda_w + (1-\phi)\lambda_s]$ of the reservoir changes as the porosity changes. The total thermal conductivity value of the reservoir increases with decreasing porosity value since the thermal conductivity of rock is much greater than that of water. This results in increase in total thermal conductivity of the reservoir. Thermal conductivity value of rock changes with respect to rock type. Hence, porosity sensitivity to temperature may increase with changing rock type. At this point, it can be understood that the sensitivity of temperature to porosity may be important especially at fall-off period if noise on temperature measurements is not so much.

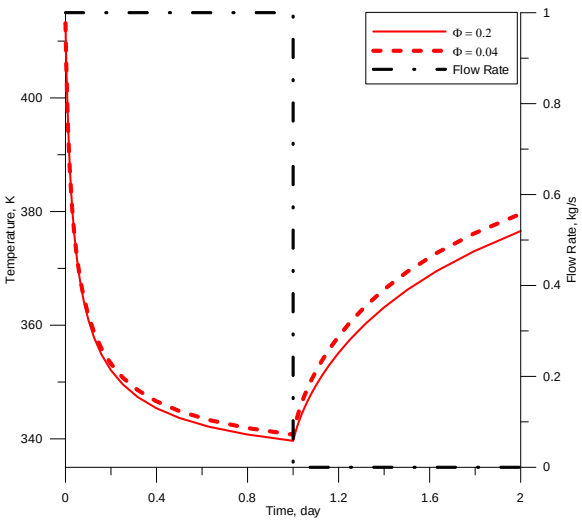

Figure 14: Effect of porosity on wellbore pressure behaviors as a function of time during injection and fall-off periods.

Packer-probe case

Here, we investigate the pressure and temperature behavior at an observation (probe) point along the wellbore due to excitation from a source/sink location (represented by a dual-packer) as shown schematically in Figure 15. Such tests (acquiring pressure and temperature measurements at the probe and dual-packer locations) are routinely applied within the context of wireline formation testing in industry to determine existence of vertical interference in the formation, estimate horizontal and vertical permeabilities and initial formation pressure and temperatures, last but not least obtain in-situ fluid samples for PVT analysis.

For this investigation, an injection-falloff test containing an injection period of 1 day and then, a fall-off (shut-in) period of 1 day. A simplified schematic of the system is illustrated in Figure 15. The pay zone has been located near the bottom of the reservoir. Like the other cases throughout the paper, it is assumed that horizontal and vertical permeabilities are also the same for this case. Dual-packer temperature response is not shown here.

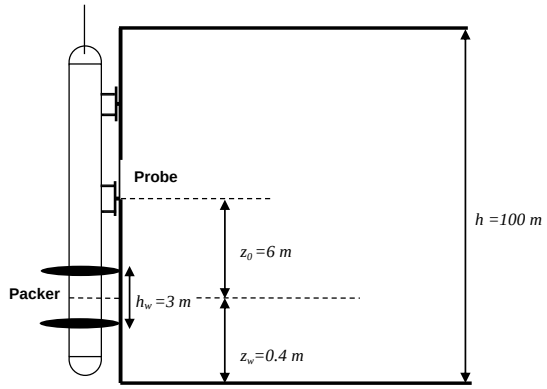

Figure 15: Schematic of a probe configuration of a packer-probe wireline formation tester for a vertical well.

Figure 16 shows pressure behaviors at the probe location in the reservoir for two significantly different values of porosity during injection-falloff periods. Since it is assumed that horizontal and vertical permeabilities are the same, then pressure for the lower porosity case has higher diffusivity both in the horizontal and vertical directions. This means that the pressure increase at probe location will be more compared to the higher porosity case.

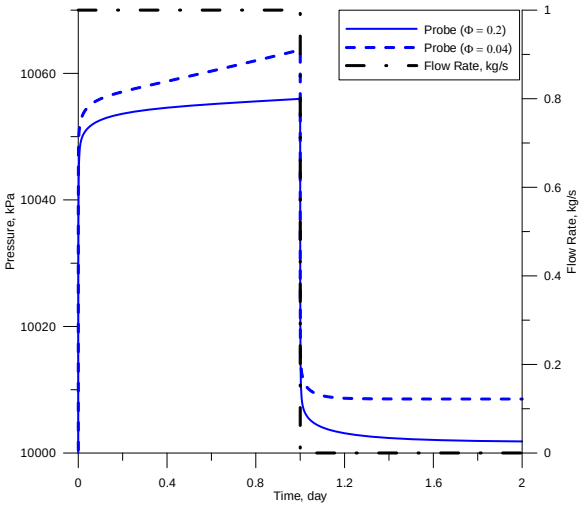

Figure 16: Effect of probe pressures to porosity during injection and fall-off periods.

Figure 17 shows the temperature behavior at the probe for two different values of porosity. At early times, spherical flow occurs at pay zone due to limited-entry. This creates a sudden cooling especially near the well at open interval to flow. The probe does not feel this cooling effect at early times because of limited-entry. Temperature drop at probe is much slower than that of packer during injection period. Hence, temperature at probe does not reach the injection temperature in contrast to that of packer.

On the other hand, probe goes on cooling during fall-off period because cooling front below probe is much closer than hot zone above it. Temperature drop in the reservoir that has greater porosity is less than that of reservoir that has lower porosity. This is because the injected fluid covers a larger volume when porosity is lower since injection is performed at constant rate. As can be seen from Figure 17, the probe temperature shows some sensitivity to porosity during injection and fall-off periods.

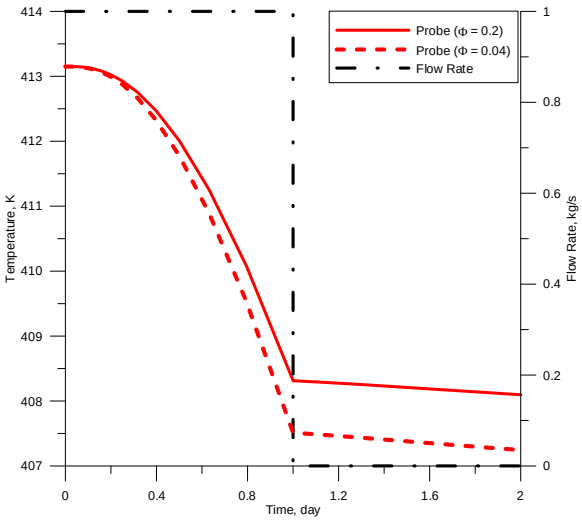

Figure 17: Effect of porosity on temperature behaviors during injection and fall-off periods.

Figures 18-21 gives 2D (*r*-*z*) temperature maps for the low porosity (0.04) case at different time steps (0.03162 days, 0.5012 days, 1 day and 2 days). It can clearly be seen that these maps also verify temperature behaviors previously explained at dual-packer and probe during injection and fall-off periods.

Sensitivity of Pressure and Temperature to Skin

In this subsection, sensitivity of pressure and temperature to skin is investigated for an injection-falloff case. The well-known Hawkins relationship is used for the treatment of the skin factor due to damage as follows:

$$S = \left(\frac{k}{k_s} - 1\right) \ln\left(\frac{r_s}{r_w}\right) \qquad (6)$$

where k_s represents permeability of skin zone and r_s represents radius of skin zone. The parameters used in modeling skin zone near the wellbore are given in Table 2.

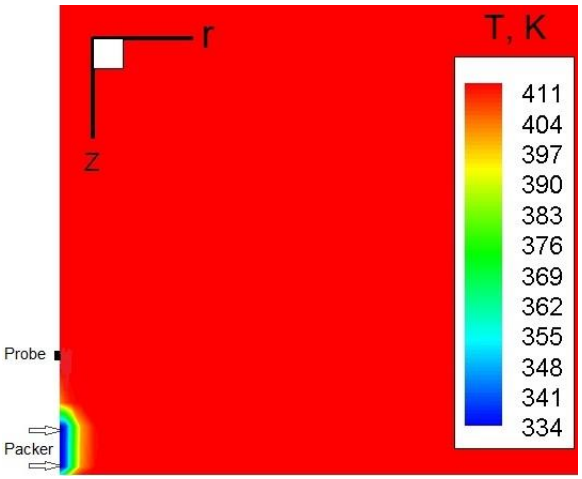

Figure 18: 2D (r-z) temperature map for the low porosity (0.04) case at dual-packer and probe at 0.003162 days of the injection period.

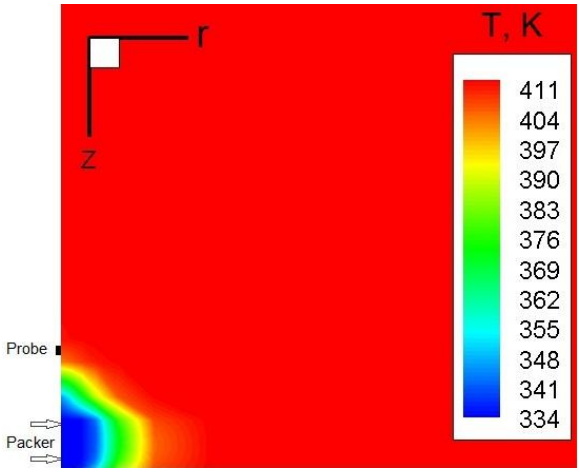

Figure 19: 2D (r-z) temperature map for the low porosity (0.04) case at dual-packer and probe at 0.5012 days of the injection period.

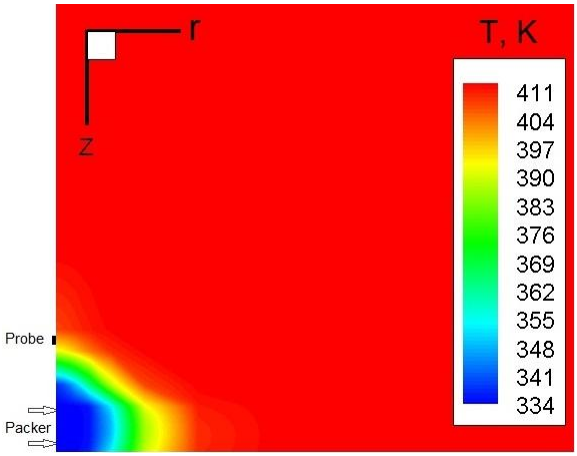

Figure 20: 2D (r-z) temperature map for the low porosity (0.04) case at dual-packer and probe at the end of the injection period (1 day).

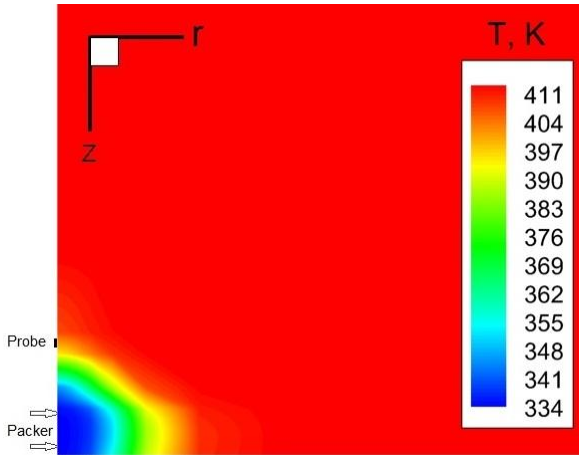

Figure 21: 2D (r-z) temperature map for the low porosity (0.04) case at dual-packer and probe at the end of the fall-off period (2 days).

Table 2: Parameters used in modeling skin zone near the wellbore.

Parameter	**Value**		
S	0	5	20
r_w, m	0.1	0.1	0.1
r_s, m	0.1512	0.1512	0.1512
k, m^2	1×10^{-13}	1×10^{-13}	1×10^{-13}
k_s, m^2	1×10^{-13}	7.5×10^{-15}	2×10^{-15}

Injection-falloff case

Figure 22 shows pressure behaviors of a fully penetrating well in the reservoir that has different skin factor values during an injection-falloff case. Increasing skin increases wellbore pressure because flow here is from well into the reservoir and resistance to flow due to increasing skin creates an additional pressure increase near the well at injection period. This is an expected behavior. All cases exhibit similar pressure drop behaviors by approximating to the initial reservoir pressure at fall-off period because the late time fall-off pressure data are independent of skin.

Figure 23 shows temperature behaviors for the same case. Note that the temperature is not sensitive to skin factor during constant rate injection and fall-off periods. This is an expected result because injection is at a constant rate. No matter what the skin is the same amount of water (and hence same amount of heat) will enter the reservoir. Although not shown here, we have observed differences in temperature in case of injection at constant bottom-hole pressure with varying skin. This is simply due to the fact that the injection rate becomes variable at constant bottom-hole pressure injection. Hence, different amounts of heat are injected for different skin.

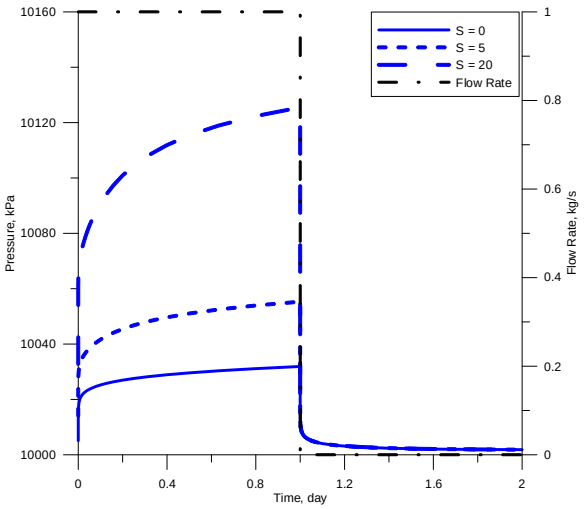

Figure 22: Effect of skin factor on wellbore pressure behaviors during injection and fall-off periods.

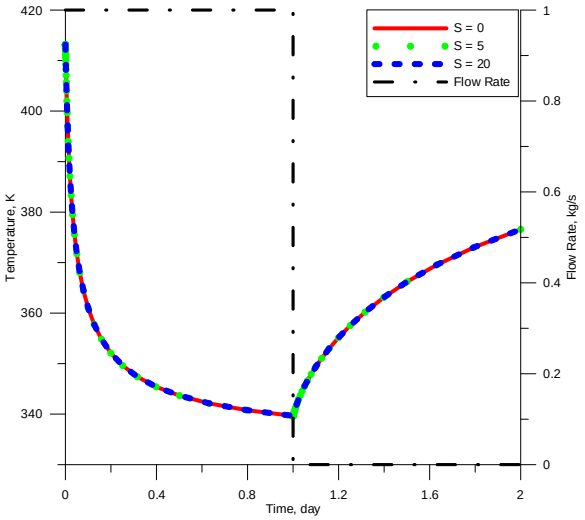

Figure 23: Effect of skin factor on wellbore temperature behaviors during injection and fall-off periods.

Effect of Limited-Entry Length on Pressure and Temperature Behaviors

In this subsection, the effect of the limited-entry length on pressure and temperature is investigated for constant-rate production and injection-falloff cases. In these cases, open interval lengths to flow are considered to be in the middle of the reservoir in z-direction.

Constant-rate production case

Figure 24 shows the effect of the length of the open interval (h_w = 1 m and h_w = 20 m) on the drawdown pressure response in comparison with the drawdown response for the fully penetrating well case ($h_w = h$ = 100 m). In these cases, differently from the fully penetrating well, more pressure drops occur due to the area open to flow is much narrower (especially for the case that h_w = 1 m). At early time, very sudden pressure drops are observed because of the limited-entry. Note that limited-entry well provides an additional (pseudo) skin effect and this results in larger pressure drop as seen from Figure 24 when h_w decreases.

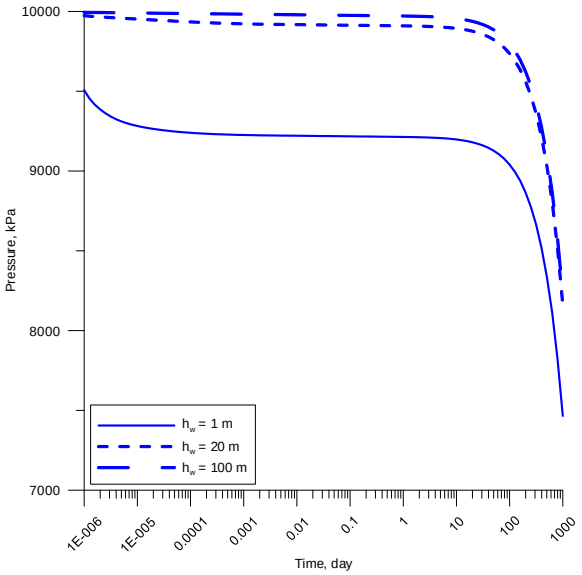

Figure 24: Effect of the open-interval length on wellbore pressure behaviors during constant rate production.

In Figure 25, we observe variations in temperature behavior. These variations occur mostly because of a combined effect of Joule-Thomson effects and expansion effects. However, it should be noted that such variations in temperature are very small and may not be easily detected by temperature sensors available today.

Injection-falloff case

Figure 26 shows pressure behaviors for wells having different open intervals to flow (from 1 m to 100 m) during an injection-falloff case. According to Figure 26, wellbore pressure increases as the open interval length decreases. This is an expected behavior because limited-entry creates a resistance to flow and hence pressure increases at a constant-rate injection period. All cases exhibit similar pressure behaviors by approximating to the initial reservoir pressure at fall-off period.

Figure 27 gives the effects of the open interval length (h_w) on temperature. At this point, it is important to note that the temperature is measured halfway through the thickness of the reservoir. For all cases of

limited-entry lengths, the rate is kept constant and the same. However, it should be noted that when the limited-entry length is increased, lesser fluid is passed through the point where the gauge is placed. This results in less cooling. Differences in temperature behavior after the shut-in period are due to the characteristics of the invaded (cool) zone created during injection.

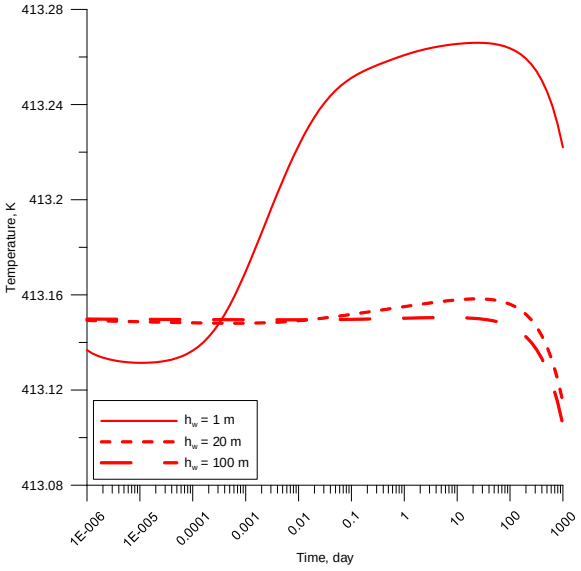

Figure 25: Effect of the open interval length on wellbore temperature behaviors during constant-rate production.

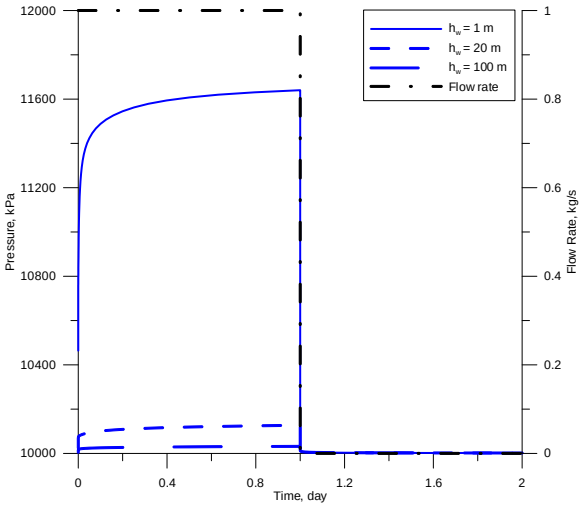

Figure 26: Effect of the open interval length on wellbore pressure behaviors during injection and fall-off periods.

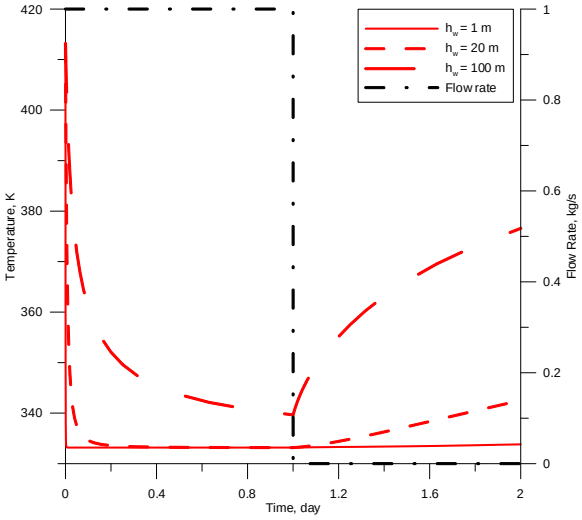

Figure 27: Effect of limited-entry length on wellbore temperature behaviors during injection and fall-off periods.

Effect of Different Injection Temperatures on Pressure and Temperature Behaviors

In this subsection, the effect of different injection temperatues on pressure and temperature is investigated for limited-entry well during constant-rate injection period. In this case, open interval length to flow (h_w = 1 m) are considered to be in the middle of the reservoir in *z*-direction. Constant-rate injection is performed at 5 different temperature values that are equal to 333.15K , 353.15K, 373.15K, 393.15K and 413.15K, respectively.

Constant-rate injection case

Figure 28 shows effect of different injection temperatures on wellbore pressure behaviors for a limited-entry well for constant rate injection period. It can be seen from Figure 28 that pressure behaviors change with decreasing injection temperature. This is caused by the fact that colder injected water has higher viscosity than that of hotter reservoir water. According to Figure 28, viscosity change of the mixed water can also be understood from more pressure increase created by injection of colder water.

Figure 29 shows temperature behaviors for the same case. According to Figure 29, temperature decreases faster with decreasing injection temperature during injection period as expected.

Sensitivity of Permeability to Pressure and Temperature Behaviors

In various injection cases performed, it is observed that permeability is sensitive to pressure while it does not seem to have significant effect on wellbore

temperature. However, it should be noted that these investigations have been performed with constant-rate production and injection. Temperature does become sensitive to permeability in cases of constant bottom-hole pressure injection.

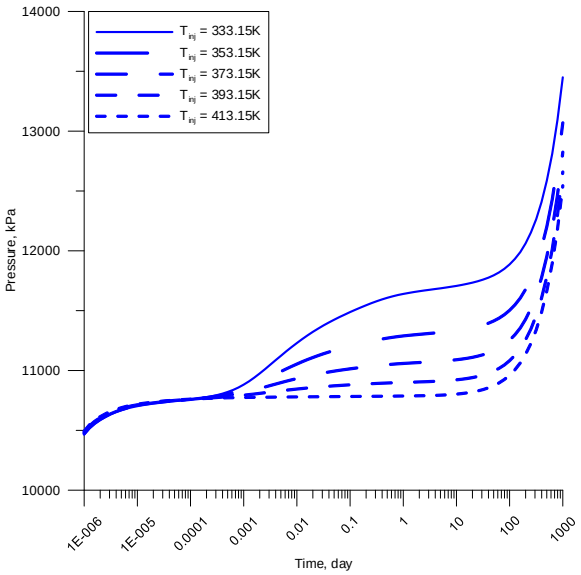

Figure 28: Effect of different injection temperatures on wellbore pressure behaviors during injection period.

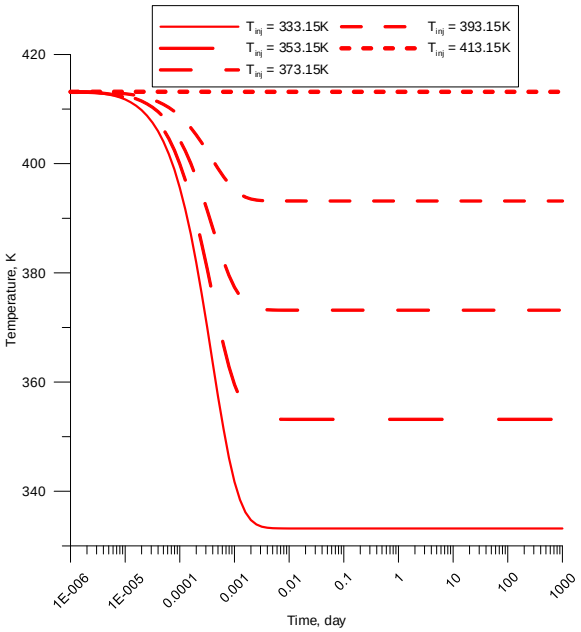

Figure 29: Effect of different injection temperatures on wellbore temperature behaviors during injection period.

CONCLUSIONS

In this study, a 2D (*r-z*) non-isothermal simulator that rigorously model wellbore pressure and temperature behaviors for single-phase geothermal reservoirs has been developed and verified by a commercial thermal reservoir simulator.

In an injection-falloff case performed for a fully penetrating well, it has been observed that temperature is significantly sensitive to rock thermal conductivity especially during fall-off period.

In injection-falloff cases performed for both fully penetrating and limited-entry wells, it has been observed that temperature shows some sensitivity to porosity especially during fall-off period.

In an injection-falloff case performed for a fully penetrated well, it has been observed that temperature is not sensitive to skin factor during constant-rate injection and the following fall-off periods due to the fact that this investigation is performed at constant-rate injection.

In a constant-rate injection case performed for a limited-entry well, it has been observed that injection of water that has different temperatures has a significant effect on pressure behavior near the wellbore due to changing viscosity values of the mixed fluids.

In various cases performed for injection, it has been observed that permeability is significantly sensitive to pressure while it does not have significant effect on temperature due to the fact that these investigations are performed at constant-rate injection.

ACKNOWLEDGEMENTS

We thank The Scientific and Technological Research Council of Turkey (TUBITAK Project No: 110M482) and the Department of ITU Scientific Research Projects for providing financial support for this study. Some portions of this work constitute the PhD study of the first author.

NOMENCLATURE

c	:Isothermal compressibility, kPa^{-1}
C	:Specific heat capacity, J/kg-K
h	:Reservoir thickness, m
h_1	:Top of open interval to flow, m
h_2	:Bottom of open interval to flow, m
h_w	:Open interval length to flow, m
H	:Specific enthalpy, J/kg
N	:Total number of grid blocks

k :Permeability, m^2
k_s :Permeability of skin zone, m^2
p :Pressure, kPa
q_m^R :Source term representing mass rate in from reservoir into wellbore, kg/s
q_z^w :Volumetric flow rate, m^3/s
$\tilde{q}$:Fourier's thermal conduction term, J/m^2s
r :Radial distance, m
r_e :Reservoir radius, m
r_s :Radius of skin zone, m
r_w :Well radius, m
S :Skin factor
t :Time, s
T :Temperature, K
U :Specific internal energy, J/kg
v :Velocity, m/s
V :Volume, m^3
z :Vertical distance, m
z_0 :Vertical distance from middle of the open interval to probe
z_w :Vertical distance from bottom of the formation to the middle of the open interval
β :Isobaric thermal expansion coefficient, K^{-1}
∇ :Gradient operator
θ :Angular direction
λ :Thermal conductivity, J/m-s-K
μ :Viscosity, kPa-s
ρ :Density, kg/m^3
ϕ :Porosity

Subscripts

i :Gridblock index for radial direction
inj :Injection
j :Gridblock index for theta direction
k :Gridblock index for vertical direction
r :Radial direction
s :Solid rock phase
sf :Sandface
t :Total system
w :Water
z :Vertical direction

Superscripts

0 :Initial condition
n :Time step
w :Well

REFERENCES

Alkan, H. and Satman, A., (1990), "A new lumped parameter model for geothermal reservoirs in the presence of carbon dioxide," *Geothermics*, 19, 5, 469-479.

App, J.F., (2008), "Nonisothermal and productivity behavior of high pressure reservoirs," SPE Annual Technical Conference and Exhibition, Denver, Colorado, USA.

Atkinson, P.G. and Ramey, H.J.Jr., (1972), "Problems of heat transfer in porous media," the SPE 52nd Annual Fall Technical Conference and Exhibition, SPE paper no 6792, Denver, Colorado.

Axelsson, G., (1989), "Simulation of pressure response data from geothermal reservoirs by lumped parameter models," Proceedings, 14th Workshop on Geothermal Reservoir Engineering, Stanford University, USA.

Bird, R.B., Stewart, W.E., and Lightfoot, E.L., (1960), "Transport phenomena," John Wiley & Sons Inc., New York.

Duru, O.O. and Horne, R.N., (2010a), "Modelling reservoir temperature transients and reservoir-parameter estimation constrained to the model," *SPE Reservoir Evaluation & Engineering*, 13, 6, 873-883.

Duru, O.O. and Horne, R.N., (2010b),"Joint inversion of temperature and pressure measurements for estimation of permeability and porosity fields," the 2010 SPE Annual Technical Conference and Exhibition, SPE paper no 134290, Florence, Italy.

Duru, O.O. and Horne, R.N., (2011), "Combined temperature and pressure data interpretation: applications to characterization of near-wellbore reservoir structures," SPE Annual Technical Conference and Exhibition, SPE paper no 146614, Denver, Colorado, USA.

Grant, M.A., Donaldson, I.G. and Bixley, P.F., (1982), "Geothermal reservoir engineering," Academic Press, New York.

Onur, M., Sarak, H., Tureyen, O.I., Cinar, M., Satman, A. (2008), "A new non-isothermal lumped parameter model for low temperature, liquid dominated geothermal reservoirs and its applications," Proceedings, 33rd Workshop on Geothermal Reservoir Engineering, Stanford University, USA.

Palabiyik, Y., (2013), "Modeling of wellbore pressure and temperature behaviors for single-phase water geothermal reservoirs," ITU Graduate School of Science Engineering and Technology, PhD (dissertation submitted in December in 2012).

Petrasim, (2011), "User manual, Version 5," Thunderhead Engineering Consultants, Rockware Inc., Manhattan, USA.

Pruess, K., Oldenburg, C. and Moridis, G., (1999), "Tough2 user's guide version 2.0," Report 476, LBNL-43134," Lawrence Berkeley National Laboratory, Berkeley, California, USA.

Ramazanov, A.Sh., Valiullin, R.A., Sadretdinov A.A., Shako, V.V., Pimenov, V.P., Fedorov, V.N. and Belov, K.V., (2010), "Thermal modeling for characterization of near wellbore zone and zonal allocation," the 2010 SPE Russian Oil & Gas Technical Conference and Exhibition, SPE paper no 136256, Moscow, Russia.

Ramey, H.J.Jr. (1962), "Wellbore Heat Transmission," *Journal of Petroleum Technology*, 14, 4, 427-435.

Sarak, H., Onur, M. and Satman, A., (2005), "Lumped-parameter models for low temperature geothermal reservoirs and their application," *Geothermics*, 34, 728-755.

Sui, W., Zhu, D., Hill, A.D. and Ehlig-Economides, C, (2008a), "Model for transient temperature and pressure behavior in commingled vertical wells," SPE Russian Oil & Gas Technical Conference and Exhibition, SPE paper no 115200, Moscow, Russia.

Sui, W., Zhu, D., Hill, A.D. and Ehlig-Economides, C, (2008b), "Determining multilayer formation properties from transient temperature and pressure measurements," SPE Annual Technical Conference and Exhibition, SPE paper no 116270, Denver, Colorado, USA.

Tureyen, O.I., Onur, M. and Sarak, H., (2009), "A Generalized non-isothermal lumped parameter model for liquid dominated geothermal reservoirs," Proceedings, 34th Workshop on Geothermal Reservoir Engineering, Stanford University, USA.

Tureyen, O.I., Sarak, H. and Onur, M., (2007), "Assessing uncertainty in future pressure changes predicted by lumped-parameter models: a field application," Proceedings, 32nd Workshop on Geothermal Reservoir Engineering, Stanford University, USA.